

—原著—

ラット骨内から摘出された純チタン製インプラントの表面分析

第2報：吸着生体分子の表面テクスチャーによる影響

渡辺孝一，大川成剛，金谷 貢

新潟大学大学院医歯学総合研究科生体材料学分野

Surface analysis of commercially pure titanium implant retrieved from rat bone.

Part 2: Biomolecular adsorption influenced by surface texture

Kouichi Watanabe, Seigo Okawa, Mitugu Kanatani

*Division of Biomaterial Science, Department of Oral Health Science**Niigata Univ. Graduate School of Medical and Dental Sciences*

平成 25 年 3 月 28 日受付 平成 25 年 4 月 9 日受理

キーワード：歯科インプラント，生体分子吸着，X線光電子分光法，プロテオグリカン，骨生成

Key words: dental implant, biomolecular adsorption, X-ray photoelectron spectroscopy, proteoglycan, bone formation

Abstract:

The relation between the surface texture (roughness) of dental Ti implants and adsorbing biological molecules has been poorly understood. To investigate the character of the adsorbing molecules at the early period, two kinds of test implants were fabricated from commercial pure titanium; they had a mirror polished surface or a grooved surface. They were inserted into rat bone, retrieved after either 3 hours or 7 days, and after cleaning analyzed with X-ray photoelectron spectroscopy. The deposition of calcium phosphate compounds was not observed on either surface. Protein adsorption was confirmed by detection of both carbon and nitrogen and the amounts of adsorbed proteins were nearly equal on the both kinds of the surfaces. Characteristic photoelectron sulfur peak (S 2p) appeared at two binding energies, 163.5 eV and 168 eV. The former was assigned to S contained in the cysteine of protein; the latter, to S of sulfate, which is mostly contained in proteoglycans. Furthermore, the amount of adsorbed proteoglycans on the polished surface was about 2 times larger than that on the grooved surface. Small pieces of new bone were observed on the grooved surface after 7 days. In conclusion, the surface texture (roughness) influences the proteoglycan adsorption, which plays a crucial role in the new bone formation.

抄録：

歯科用チタンインプラントの表面特性（粗さ）と生体内でその表面に吸着する分子との関係についてはほとんど知られていない。生体内埋入の初期における吸着分子の特性を解明するため、2種類の実験用インプラントを市販されている純チタンから作製した。その試験面は鏡面研磨されているかまたは鏡面研磨の後溝加工されている。各インプラントはラット骨内に埋入され、3時間後または7日後に取り出され、超音波洗浄した後にX線光電子分光装置により分析された。いずれの処理面においてもリン酸カルシウム化合物の付着は認められなかった。炭素と窒素のピーク強度からタンパク質の吸着が確認され、その吸着量に関しては2種類の処理でほとんど差は認められなかった。検出されたイオウのピークは2種類の結合エネルギー、163.5 eV と 168 eV に分かれて存在した。前者はタンパク質を構成しているシステイン内のイオウに帰属され、後者は硫酸基に帰属された。プロテオグリカンは多数の硫酸基を含むことが知られている。鏡面でのオプロテオグリカンの吸着量は溝加工された表面のおよそ2倍であることが示された。更に、新しい骨の生成が溝加工された面で確認された。以上の知見より、表面特性（粗さ）はプロテオグリカンの吸着量に影響し、そのことが骨生成に関して重要な役割を演じていると結論される。

INTRODUCTION

Dental implants are used to replace missing teeth by anchoring prostheses to the mandible or maxilla. Among many implant types, the most successful single-tooth implant is a screw-type implant made of commercial pure titanium¹⁾ (cpTi, hereafter simply Ti). This clinical success, osseointegration, could be largely attributed to the excellent biocompatibility exhibited by Ti, which more basically is attributed to both properties, the surface texture¹⁾ of the implant and chemical properties of native titanium oxide layer²⁾.

Based on many *in vitro* experimental results^{3, 4)}, it was believed that calcium phosphate compounds, such as hydroxyapatite, deposited on Ti surface from a physiological solution contributed mainly to its excellent biocompatibility. The *in vivo* experiment⁵⁾, however, in which the implant having a sandblasted surface was retrieved after 7 days from rat bone, indicated that such compounds were not observed on the Ti surface. This finding implies that the deposition of calcium phosphate compounds did not take place under the *in vivo* environment and therefore was not responsible for the excellent biocompatibility of Ti. Instead, the adsorption behavior of biomolecules, such as proteins, is expected to be a crucial factor for the biocompatibility.

Early biological responses to implant surfaces are known as follows⁶⁾: Within nanoseconds, a water monolayer is formed, followed by adsorption of small molecules, such as amino acid and glucose. Proteins adsorption is initiated within a few milliseconds of contact with biological fluid. Competitive adsorption usually occurs; the molecules that have stronger attractive force to the surface are adsorbed by interchange with weak interaction molecules such as small molecules. This exchange is known as the Vroman effect⁷⁾. It is noteworthy that biological macromolecules include not only proteins but also glycoproteins, glycolipids, lipoproteins, proteoglycans, polysaccharides, and so forth⁸⁾. Living cells and the implant surface do not directly contact; rather they contact through the medium of the adsorbed molecules on the implant. This is the reason why the adsorption behavior is critically important to understand the biocompatibility.

The surface roughness of Ti implant is one of the

crucial factors for the clinical success¹⁾. Clinically it is well known that the implants having about ten micron roughness have been favorable for both bone anchoring and biomechanical stability⁹⁾. As for the effects of micro-fabricated surfaces on bone formation, Brunette *et al*¹⁰⁾ carried out systematical studies, *in vitro* and *in vivo*. They pointed out that surface texture influenced the amount of bone deposition adjacent to implants and that mineralized product could be guided by the surface texture. In this manner, many *in vitro* studies have demonstrated that a microscopically modified titanium surface can influence cell responses. However, the precise role of the roughness on the early bioresponse, such as biomolecular adsorption, has remained unclear⁹⁾. In other words, the basic question, why the Ti implant having ten micron surface roughness is favorable for osseointegration, has not been solved yet.

For biocompatibility of Ti, most researchers have focused on adsorption of only protein as biological responses¹¹⁾, but many other biomolecules, such as proteoglycan, probably should play some role as biological responses⁸⁾. Proteoglycan is a high molecular weight polyanionic substance covalently linked by numerous hetero-polysaccharide side chains to a polypeptide chain backbone and plays a certain role for bone formation¹²⁾. In early days, Linder *et al.* pointed out the existence of this molecule at the bone-titanium interface¹³⁾. Recently, Nakamura *et al.* discussed a role of proteoglycans in mineralized tissue-titanium adhesion¹⁴⁾. Moreover, they pointed out that the potential role of proteoglycans associated with roughened titanium surfaces had rarely been investigated.

Another important but poorly understood factor for bone formation is Si, whose concentration is appreciably high level in human blood¹⁵⁾. Furthermore, connective tissues tend to have a high Si content, mainly because Si is an integral component of glycosaminoglycans and their protein complexes, which contribute to the tissue structures. Although Si has been shown to be localized in active calcification sites in young mouse and rat bone, it remains a relatively unknown trace element¹⁵⁾.

The purpose of this study is to elucidate adsorption behavior on the implant surfaces having different textures *in vivo*, and to investigate the role of the adsorbed molecules for biocompatibility and the bone

formation.

MATERIALS AND METHODS

Implant fabrication having two types of surface textures

A bullet type Ti implant, 1.1 mm in diameter and 3.5 mm in length, with a flat area on the lateral surface was used. The flat area (test portion) of every sample was at first polished with an automatic polisher (Auto Max, RefinTec, Yokohama, Japan) with silica slurry of mean grain size of $0.06 \mu\text{m}$; this was called as the polished surface hereafter. The polished implant means that the whole flat is mirror polished surface. The grooved implant means that the center area of the polished surface was fabricated by machining with fly cutting using diamond tool. This texture was V-shape groove with 90 degrees and $10 \mu\text{m}$ in depth. The grooved implant was shown by secondary electron (SE) image of the flat area (Fig.1). The grooved area appears bright because of many secondary electron from the surface. As shown in Fig.1, the tip and the tail of the bullet implant were remained polished. Before implantation, every implant was rinsed with acetone in an ultrasonic cleaner for 5 minutes, followed by Ar sputter etching (radio frequency type) for 5 minutes at 100 W. The last treatment was carried out for both a sputter cleaning step and a sterilization treatment.

Implantation procedure and cleaning of the retrieved implant

Femurs of 8-week-old male Wistar rats were used in this study. Most procedures were the same as noted in previous paper¹⁶⁾. The bone cavities (1.15 mm in diameter, 3 mm in depth) were prepared for implantation by drilling with an engine reamer and a drill (Peeso drill, Maillefer Co. LTD, Ballaigues, Switzerland). The implant was inserted into the cavity by tapping with a mallet. As illustrated in Fig.2, the bullet bottom was kept 0.5 mm from the cortical bone. No antibiotics were given. The implants were retrieved after either 3 hours or 7 days.

All the animal experiments in this research were done following the Niigata University Guidelines for Animal Experimentation.

To remove the molecules and organisms loosely bound to the implant surface, all the retrieved implants were washed for 4 minutes in ultra-pure water with

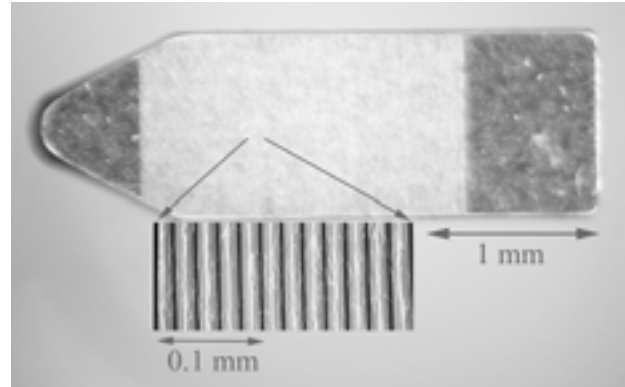


Fig.1 SE image of a grooved surface; low magnification picture having partly high magnification area
The center area of the polished surface was fabricated to V-shape groove (appearing brightly) by machining with fly cutting using diamond tool.

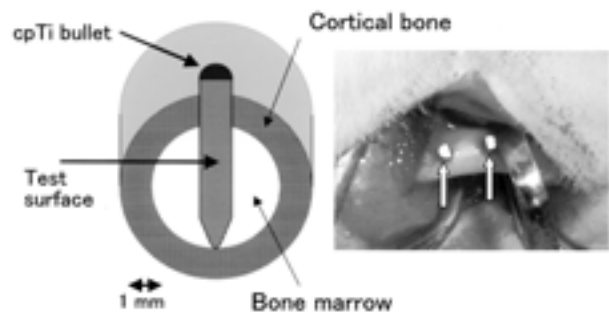


Fig.2 Schematic representations and the picture of the rat femur after Ti bullet implantation
Test surface was flattened to prevent rubbing against the bone wall when extraction of the implant. In the right side, the two white arrows indicate the inserted implants.

an ultrasonic cleaner. Thereafter, they were quickly dried up and stored in a vacuum container. Three implant samples were tested under each texture condition.

X-ray photoelectron spectroscopy (XPS)

X-ray photoelectron spectroscopy (XPS) (Quantum 2000, ULVAC-PHI, Tokyo, Japan) was used to examine the flat surfaces of retrieved implants under these conditions: monochromatic Al K α (1487 eV) X-rays at 25W, spot size of $100 \mu\text{m}$, and take off angle of 45 degrees. Survey spectra were obtained over a range of 0-1000 eV with a path energy of 46.9 eV. High resolution spectra of the peaks, such as C 1s, O 1s, Ca 2p, and P 2p, were also collected. In addition, to obtain S 2p peaks with high confidence, XPS high power mode (100 W) was used. These XPS measurements

were carried out in a domain of the 2.5 mm inside from the edges of the retrieved implants in order to avoid influence of an edge. The XPS measurement at the new bone was exception because new bones were observed only near the edges.

From the change in Ti intensity before and after implantation, the thickness of the covered layer on the implant surface was evaluated⁵⁾. In the process of the estimation, the inelastic mean free path (IMFP) value of 3.16 nm (at Ti 2p_{3/2}; electron kinetic energy is 1032 eV) was adopted, which was calculated by Tanuma *et al.*¹⁷⁾ for the bovine plasma albumin (BPA). As for the grooved samples, the take-off angle (90 degrees) of the photoelectron detector to their surface were different compared to that (45 degrees) to the polished samples, and hence, correction of the adsorption layer thickness had been performed by considering the angle difference.

Calcium and phosphorus quantitative measurements were carried out by means of peak area of XPS high resolution spectra. The quantitative measurements of two types of S 2p binding energies were estimated by peak deconvolution software.

For XPS depth analyses of Si, they were carried out by means of Ar sputter etching. The sputter conditions were: accelerating voltage was 0.5 kV, the sputtering area was 4 mm², and the sputtering time was 1 minute. Under these conditions, the sputtering rate was equivalent to that of 0.5 nm/min for SiO₂.

Statistical analysis

For the quantitative data of adsorption layer thickness, Ca/P atomic ratios and intensities of two types of sulfur, the differences between the mean intensities in the implantation periods or difference in surface treatments were statistically analyzed using Student's t-test at a significance level of $p = 0.05$.

For the data obtained from multi-point measurement mode, they were analyzed by scatterplot and Pearson-moment correlation coefficient¹⁸⁾. In addition, for the purpose of visualization, regression line was drawn in each scatterplot.

RESULTS

Figure 3 shows the part of the magnified typical survey spectra of the samples before implantation (after cleaning by Ar sputter etching). Elements, Ti,

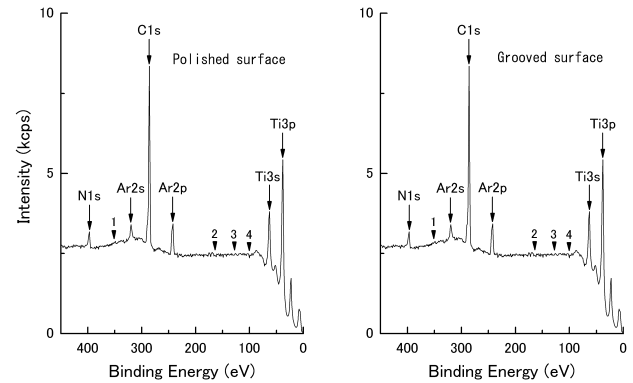


Fig.3 XPS survey spectra (part) of cleaned implants before implantation, polished surface and grooved surface. Each arrowhead with number indicates the peak position (not detected): 1; Ca 2p (350 eV), 2; S 2p (165 eV), 3; P 2p (130 eV), 4; Si 2p (99 eV).

Ar, and C peaks were mainly detected and a small peak of N was recognized. Ar atoms were detected because of sputtering treatment¹⁹⁾. Carbon was the contaminant that usually adsorbed from atmosphere. Some amounts of O also were detected but the peak did not present in this energy extent. Arrows in the figures were attached to the peak positions of the important elements related to adsorption molecules: 1; Ca 2p (350 eV), 2; S 2p (165 eV), 3; P 2p (130 eV), 4; Si 2p (99 eV).

Figure 4 shows the typical XPS survey spectra of the mirror polished surface; after 3 hours (a) and 7 days (b) of implantation. The spectrum (a) was shifted upward to avoid overlapping, but the horizontal scale is common to both spectra. Ti peak of 7 days implantation was larger than that of 3 hours implantation. This suggests that the adsorption film of 3 hours implantation is thicker. The other peaks were similar for both spectra. The peaks of O, C, and N were clearly observed. Si 2s peak was also clearly observed. The peaks of Ca, S, and P were very small.

Figure 5 shows the typical XPS survey spectra of the grooved surface; after 3 hours (a) and 7 days (b) of implantation. The demonstration form is the same as that of Figure 4. The both spectra were similar to those in Fig.4, but the peaks of Si were markedly smaller than those in Fig.4.

Figure 6 shows the film thickness formed on the implant surface in relation to implant periods and surface treatments. There was significant difference between the implant periods, 3 hours or 7 days. However, there was no significant difference between

the two textures, the polished surface and the grooved surface.

Figure 7 shows the Ca/P atomic ratio on the two types of textures and implantation periods. Each Ca/P atomic ratio was calculated based on the intensity ratio and the atomic sensitivity factors (Ca = 1.833, P = 0.486)²⁰⁾. There was a tendency that the ratio decreases with the increase in implant interval but there was no significant difference. It is remarkable that all the Ca/P atomic ratios were very small (0.2 or 0.3) than those expected from calcium phosphate compound, including hydroxyapatite (1.7).

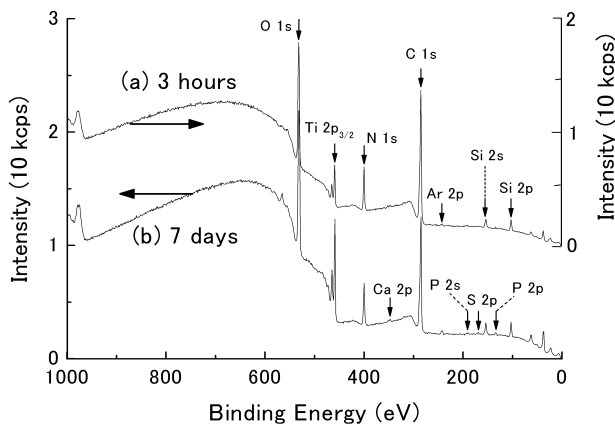


Fig.4 XPS survey spectra of the polished surface of the implant extracted from rat bone

To avoid overlap of the spectra, one of two was shifted up, where the intensity was shown by the right vertical axis. To avoid overlap of the notations, peak notations were attached to one of two spectra.

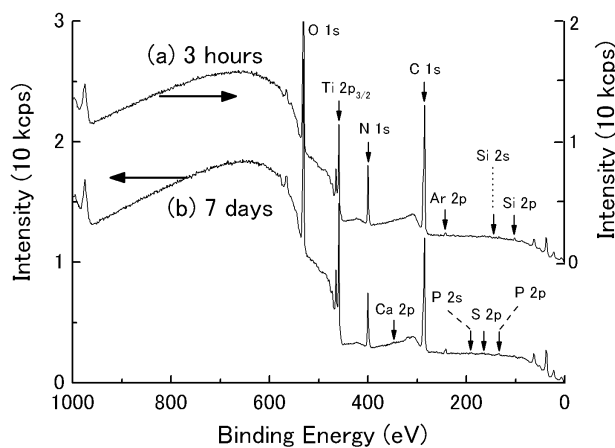


Fig.5 XPS survey spectra of the grooved surface of the implant extracted from rat Bone

To avoid overlap of the spectra, one of two was shifted up, where the intensity was shown by the right vertical axis. To avoid overlap of the notations, peak notations were attached to one of two spectra.

Figure 8 shows all the XPS high resolution spectra (nine spectra of each texture) of S peaks of the implants after 3 hours of implantation: the polished surface (upper) and the grooved surface (down). Two peaks having binding energies, 163.5 eV and 168 eV, were recognized. Considering the published data, the former was assigned to sulfur contained in the cysteine^{21, 22)}, and the latter, to sulfur contained in sulfate^{21, 23)} of organic compound. The peaks at 168 eV showed markedly difference between the surface treatments.

Figure 9 shows the mean peak intensities of two binding energies of S 2p. As for the peak intensity at 168 eV, there was significant difference between the

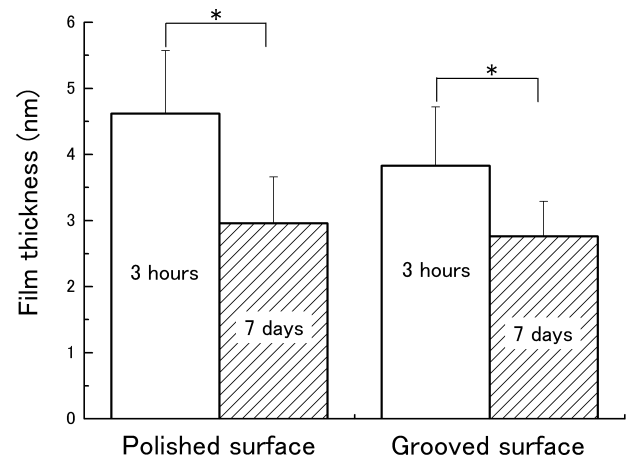


Fig.6 The film thickness on the implant surface of each characteristic surface

An asterisk indicates statistically significant difference ($p < 0.05$ by Student's t-test) between implant periods.

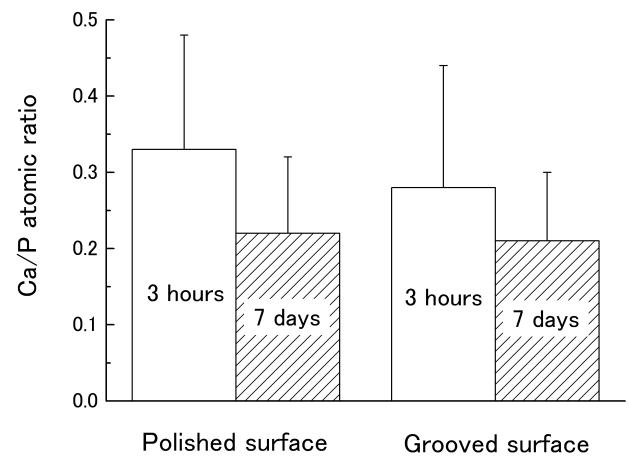


Fig.7 Ca/P atomic ratio on the implant surface of each characteristic surface

No significant differences were observed between implant periods as well as surface treatments.

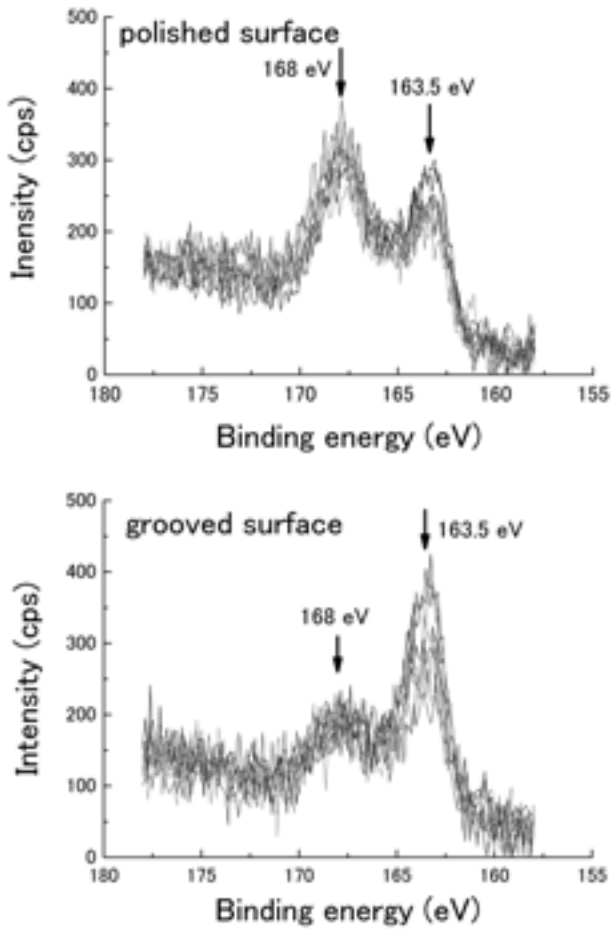


Fig.8 XPS high resolution spectra of S 2p peaks after 3 hours implantation on the polished surface (upper) and the grooved surface (bottom) Spectra were obtained at three areas of each implant. Accordingly, nine spectra were shown for each surface treatment.

surface treatments: the intensities on the grooved surface were about half in comparison with those on the polished surface. However, there was no significant difference between implantation periods of each treated surface.

The XPS element maps in Fig.10 show the intensity distributions of S 2p (168 eV), S 2p (163.5 eV), N 1s, and C 1s, on the polished specimen retrieved after 3 hours. All the measurement points were 2.5 mm inside from the edge. In each map, the relative intensities are indicated by the pseudo color: white (the highest intensity), yellow, orange, red, blue, and black (the lowest intensity). The highest and the lowest intensities (counts) of each map were different, and therefore, the intensities were noted in parentheses together with the element; (S 2p at 168 eV; 183, 66), (S 2p at 163.5 eV; 147, 0), (N1s; 6934, 3055), and (C 1s;

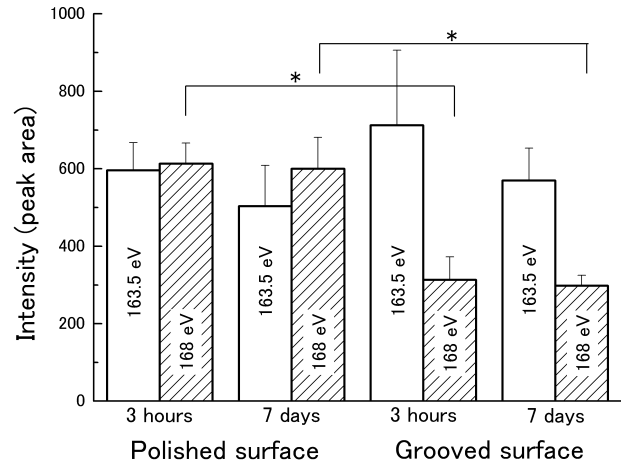


Fig.9 Mean intensity estimated from peak area of two types of S 2p binding energy; on the polished surface and the grooved surface. An asterisk indicates that the intensities of S 2p peak at 168 eV were statistically significant difference ($p < 0.05$ by Student's t-test) between the polished surface and the grooved surface.

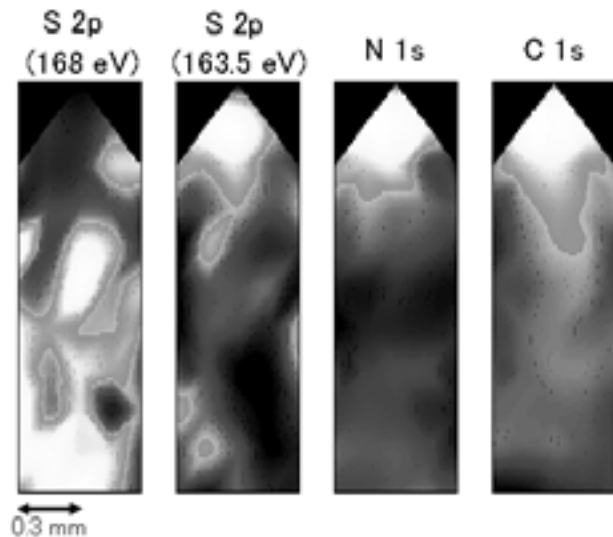


Fig.10 Distribution maps of S 2p at 168 eV, S 2p at 163.5 eV, N 1s, and C 1s peak intensities of the polished sample after 3 hours. In each map, the steps of intensity are indicated by the pseudo color; the white (highest), yellow (secondly highest), red (medium), blue (low).

25300, 17200). Three maps, the S 2p (163.5 eV), N 1s, and C 1s, showed the distributions similar to each other, confirming that the S 2p at 163.5 eV came from cysteine included in proteins. On the other hand, little correlation was observed between the distribution of S 2p (168 eV) and those of the other three.

Figure 11 shows the scatterplot of Ca 2p intensity versus S 2p intensity at 168 eV on the polished surface

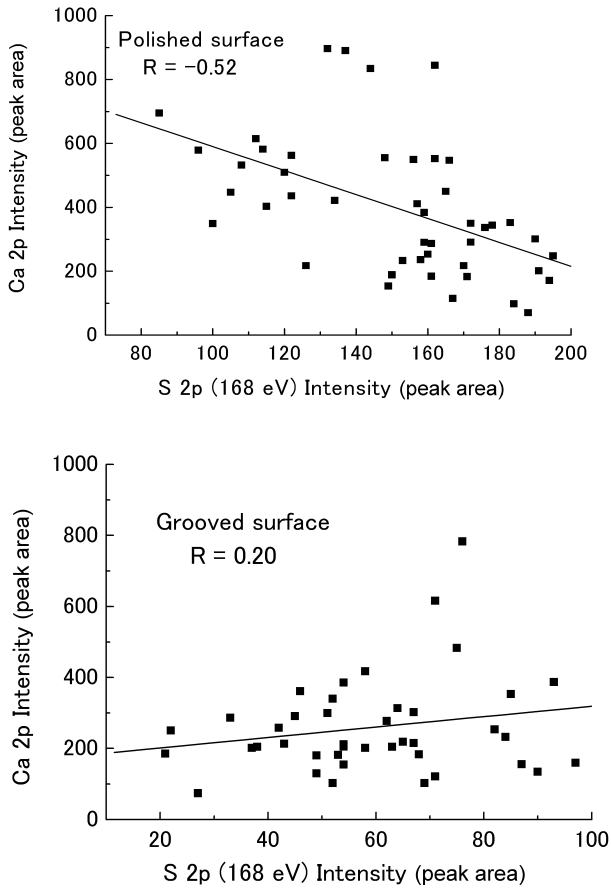


Fig.11 The relationship between S 2p intensity at 168 eV (horizontal axis) and Ca 2p intensity (vertical axis); scattered plot
These intensities were obtained from the multi-points analysis on the polished surface (upper) and the grooved surface (bottom). Each correlation line was indicated in the respective figure.

(upper) or the grooved surface (bottom); these data were obtained from the multi-points analysis on the polished surface (upper) and on the grooved surface (bottom). The Ca atoms were expected to be comprised of both ones adsorbed on the Ti surface and ones bound to the sulfate. As for the polished surface, moderate negative correlation was observed, suggesting that most Ca existed as adsorbed ones. Contrarily, on the grooved surface, a weak positive correlation was observed, indicating that significant quantity of Ca was bound to the sulfate group ($-\text{OSO}_3$).

Figure 12 shows Si 2p peaks of various levels of depth obtained from the polished surface after 7 days' implantation. At the outermost surface, S 2p binding energy was 103.5 eV, which was assigned to the Q type of siloxy, quaternary $[\text{SiO}_{4/2}]^{24)}$. With Ar sputtering, the peak gradually decreased and shifted

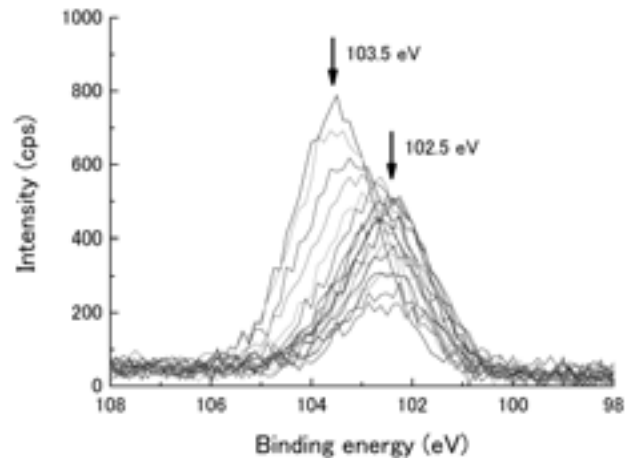


Fig.12 XPS Si 2p spectra at various depth obtained from depth profile measurement of the polished surface (7 days implantation)
The peak at 103.5 eV was obtained from the outermost surface, and it shifted gradually to 102.5 eV.

to the lower binding energy, 102.5 eV, which was corresponding to the T unit of siloxy, tri $[(\text{CH}_3)\text{SiO}_{3/2}]$. The Q and T siloxy units are constituents (silanolate) included in complex polysiloxane systems. The sputter etching rate was estimated to be 0.3 nm per minute from the data of the adsorption layer thickness and the decrease of N signal⁵⁾. This means that the Q type of siloxy was present till depth of 1.2 nm from the outermost surface.

Figure 13 shows the SEM image of the area of the implant retrieved after 7 days, in which the inclined arrow indicated the edge of the implant. The XPS narrow spectrum obtained from the particle indicated by the arrow head was presented in bottom. Both peaks, Ca and P, were very strong, and the atomic ratio Ca/P was 2.0. In addition, carbonate peak was detected by means of the deconvolution technique of the C 1s peak. Small but appreciable Si peak was observed.

DISCUSSION

Confirmation of surface cleanness

Before implantation, every implant was cleaned by Ar sputter etching. This effectiveness was confirmed by the XPS spectra in Fig.3. Elements, Ca, S, P, and Si, which were all important for investigating the initial biological response, had been completely eliminated. Accordingly in the following experimental results, we

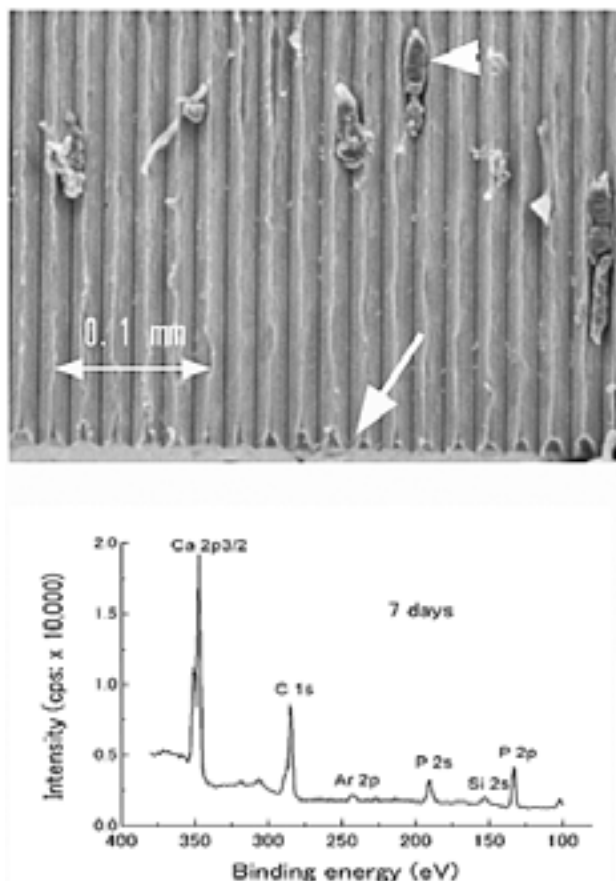


Fig.13 SEM observation of the portion where new bone was recognized (upper), and the XPS spectrum (down) at one of new bones shown by the arrow head
The inclined arrow indicates the edge of the implant.

need not consider the difference in chemical composition of the surfaces fabricated in different manners.

Moreover as for the retrieved implant from the rat bone, ultrasonic cleaner was performed for 4 minutes, by which the molecules and organisms loosely bound to the surface were removed. This procedure enabled us to analyze the true interface between the implant and biological environment. The evidence that the substrate element, Ti and Ar, were detected in XPS spectra (Fig.4 and Fig.5) proved the existence of only very thin layer on the surface.

The adsorption character 1; layer thickness and Ca/P atomic ratios

After implantation, the XPS survey spectra indicated that main elements relating to the adsorbed layer were C (including small amount of contaminant) and N

(Fig.4 and Fig.5) regardless of the implant intervals. This indicated that the layer was composed of the biomolecules including proteins, proteoglycans, and so on⁸⁾.

The thicknesses of the adsorbed layers were from 3 nm to 5 nm. This result suggests that the adsorption layer was a monolayer of biomolecules because the diameter of most globular proteins is from 2 to 7 nm²⁵⁾. In this case, attention should be paid to calculation background, because the value of 1.14 g/cm³ was adopted as the density of BPA¹⁷⁾. If the density of the adsorption layer was half of the value, the thickness of the layer became two times.

There was significant difference between the implant intervals (Fig.6); approximately 4 nm after 3 hours and 3 nm after 7 days. That is, decreasing in layer thickness with the implantation period was found for both textures. The amount of the adsorbed protein, which was estimated from S 2p at 163.5 eV in Fig.9, showed slightly decrease with time, but the change was not significant. Furthermore, the amount of the proteoglycans was almost equal for both periods. Accordingly, decreasing in layer thickness (Fig.6) with the implantation period was probably due to the orientation change of the adsorbed molecules. In addition, the decrease is not due to the deformation into their oblate shapes. This is because the structure of globular protein native state is very closely packed and therefore relatively rigid; the proportion of space occupied by the component atoms is about 75 %, being comparable to 74 % for crystals of simple organic molecules²⁶⁾.

The Ca/P atomic ratios on the implant surface were very small (less than 0.4) in comparison to those of the calcium phosphate compounds, such as HA (1.7). This was consistent with the results reported previously^{5, 27)}. The finding indicated that no calcium phosphate compounds were formed on the titanium surface *in vivo* in 7 days. Accordingly, the deposition of calcium phosphate on the Ti cannot be the reason of its excellent biocompatibility.

The adsorption character 2; two binding energies of sulfur

As seen in Fig.8, S 2p peak was composed of two peaks (two binding energies); 163.5 eV and 168 eV. As noted previously, the former was assigned to the cysteine in proteins. In general, the percent occurrence

of cysteine in average protein is not frequent and the second smallest in 20 amino acids, 1.7 %²⁸⁾. One of the probable candidates of the protein is the bone morphogenetic protein (BMP), because members of BMP subfamily show an identifying pattern of seven conserved cysteine residues in the mature, carboxyl-terminal portion²⁹⁾. Another candidate of cysteine-rich proteins is metallothionein that contains about 30 % cysteine³⁰⁾, and that is potentially involved in zinc homeostasis. In this case the possibility of metallothionein is low because coexisting metals were not detected. Therefore, the intensity of S 2p at 163.5 eV represented the amount of proteins, mostly BMP.

As for the latter binding energy, it was assigned to the sulfur in sulfate ($-\text{OSO}_3^-$; 168 eV). It is known that the proteoglycan includes a large amount of $-\text{OSO}_3^-$ groups and has been detected at the interface of titanium implant and tissue^{13, 14)}. In addition, proteoglycans bear greater than 95% of the sulfate groups within any organic matrix¹²⁾. Therefore, observed $-\text{OSO}_3^-$ groups are regarded as originating from the proteoglycans.

Relationship between surface roughness and adsorbed molecular types

The relationship between the surface roughness and adsorbed biomolecules is summarized by considering Fig.9, as follows: The amount of adsorbed proteins did not change substantially, regardless of the difference in surface roughness. That is, even if the roughness was either nano-meter order or micron-meter order, the surface roughness did not have an influence on the adsorption behavior of proteins.

In contrast, the amount of proteoglycans on the polished surface was definitely dependent on the surface roughness. This particular behavior will be attributed to its structural character.

The character of proteoglycan and its behavior for adsorption

The proteoglycan is characterized by the covalent attachment of long chain polysaccharides (glycosaminoglycans, GAGs) to core protein molecules¹²⁾ and bears a large amount of sulfate (negative charges). Proteoglycan aggrecan has a mass of about a few mega Daltons with over 100 GAG chains and its size exceeds the order of a few micrometers. In addition, GAG chains are too stiff to

fold up into the compact globular structures³¹⁾. Therefore, they are molecules extending to large areas. Because of these characters, they will be adsorbed to the Ti surface in different manners dependent on the surface texture.

In the case of the polished surface, the proteoglycan binds strongly to the Ti surface by the mainly electrostatic force of sulfate: Most sulfate sites came very close to the surface, so that the total electrostatic force exerted strongly. On the grooved surface, however, only the part of sulfate sites came close to the surface because of stiffness of the molecule, and therefore, the total electrostatic force weakly contributed to the adsorption.

Adsorption energy and stay time on the surface

The relationship between attractive force and average stay time, of adsorbed chemical species is known as follows³²⁾:

$$\tau = \tau_0 e^{U/RT}$$

where τ_0 is the constant of order of 10^{-13} sec, U is the adsorption energy, which is corresponding to the attractive force, R is the gas constant and T is the absolute temperature; the RT equals about 2.5 kJ/mol at a room temperature. If the U is considerably larger than 2.5 kJ/mol, then the average stay time is estimated to be long. Therefore, the stay time of proteoglycan on the polished surface is expected to be significantly long because of its very strong attractive force caused by its extremely large molecular weight and many sulfates. The surface concentration (coverage ratio), which is determined by XPS, is influenced by collisions of the molecules per unit time as well as average stay time.

The large adsorption energy of proteoglycan is caused by a large amount of negative charges (sulfate ion) included in the molecule itself. In the case of interaction between electric charge and metal, the method of images³³⁾ can be applied. The method of image charges (also known as the method of mirror charges) is a notion in electrostatics and is defined as follows. When a test (real) charge comes near a metal, it induces surface charge that is distributed in a complicated way. However, this is simplified to the problem of the interaction between the real charge and the imaginary charge (equal in magnitude and opposite in sign) located at the mirror image point behind the surface defined by the position of the

metal³³⁾. Moreover, the closer the real charge comes to the metal surface, the greater becomes the magnitude of the short-range image interaction (attractive force). The distance at which the short-range image forces start to become significant is on the order of 10 nm³⁴⁾. Considering that adsorption layer was about 4 nm thickness (Fig.6), this large interaction energy is expected to be dominant for proteoglycans on the polished surface.

Contrarily, in the case of the grooved surface, the average distance between the proteoglycan and the titanium surface was large compared to that of the polished surface, and accordingly the total interaction energy for adsorption, U , of the molecule was relatively small. As a result, the surface coverage on the polished surface was larger than that on the grooved surface. This is the reason why the quantity of the proteoglycan on the polished surface was large compared to that on the grooved surface. This is why the intensities of S 2p peak at 168 eV (originated from proteoglycan) of the polished surface were significantly higher than those of the grooved surface (Fig.9).

Although the proteoglycans are known to be highly water-soluble³¹⁾, some amounts of those on the Ti surface were observed after 4 minutes ultrasonic cleaning in pure water. This fact supported the strong interaction between the proteoglycan and the Ti surface. In addition, Nakamura *et al.* reported that the various GAG/proteoglycan complexes were localized at the tissue-titanium interface, which was not seen clearly at the tissue-polystyrene interface¹⁴⁾. Their result also supports our discussion where the proteoglycans interact to the substrate surface by electrostatic force, for the interaction of the proteoglycan to titanium (metal) is strong but is weak between the proteoglycan and polystyrene (insulator).

The role of the proteoglycan for bone formation

It is known that proteoglycans fulfill a variety of biological functions, such as growth factor concentration, growth modulation, ionic filtration, and cell adhesion³⁵⁾. In addition, it is also known that cartilage glycosaminoglycan functions as a reservoir of Ca for calcification of epiphyseal cartilage³⁶⁾. On the polished surface (Fig.11, upper), the function of Ca reservoir was not observed. This finding is given from the result that Ca intensities had a moderately negative correlation to the sulfate (S 2p; 168 eV)

intensities. That is, most Ca atoms existed not at sulfate sites (outermost layer), but as the adsorbed species on the Ti surface (beneath the adsorbed proteoglycan). The reason why Ca ions did not link to the sulfate on the polished surface, is that each negative charge of the proteoglycan bonded with its mirror charges (positive charge) very strongly, and hence, Ca ions could not bond with the sulfate. In conclusion, proteoglycan on the polished surface did not reserve Ca ions and hence the presence of proteoglycan does not necessarily facilitate bone formation.

In the case of the grooved surface, weak positive relation was observed between amount of Ca and sulfate intensities (Fig.11, bottom). This fact indicates that there were two types of Ca, one was adsorbed on the metal (negative correlation) and the other was bonded to the proteoglycan (positive correlation). In other words, proteoglycans on the rough surface enable to act as a reservoir of Ca. This reason is that some of the sulfate group existed at markedly long distance (longer than 10 nm) from the Ti surface beyond the working distance of the mirror force, and in this case, the sulfate bonded with not its mirror charge but Ca ion. In conclusion, proteoglycan on the grooved surface was expected to facilitate bone formation.

Therefore, proteoglycan plays two kinds of roles concerning bone formation: One is facilitating new bone formation in the case of the Ti surface with a few micron meter roughness and the other is inhibiting it in the case of Ti with the polished surface.

The role of silicon for the bone formation

As seen in Fig.4, some amounts of Si were detected on the polished surface, but only small amounts were detected on the grooved surface (Fig.5). Schwarz³⁷⁾ reported that silicon was found to be constituent of certain glycosaminoglycans and polyuronides, where it occurs firmly bound to the polysaccharide matrix. In our results, the positive correlation between the amount of silicone and the amount of proteoglycan was observed, being consistent with his result. In addition, the amount on the outermost layer, Q unit (103.5 eV) of siloxy was observed and just below the layer, T unit (102.5 eV) was detected (Fig.12). These findings supported also his prediction that Si might be present as a silanolate. However, the role of Si on bone

formation needs further study.

The new method for estimating biocompatibility

As one of the application of this research, we offer the new method that enable *in vivo* assessment of the surface roughness of a Ti implant. By means of the XPS analysis on S 2p intensities, the ratio of the peak at 168 eV to that at 163.5 eV indicates the criterion of the biocompatibility regarding surface roughness. Under the same chemical conditions, the smaller ratio implies more favorable roughness for bone formation. This method based on this experimental evidence has two major advantages; one is *in vivo* assessment and the other is very short implantation period, only 3 hours.

CONCLUSIONS

Results of this study demonstrated the following biological responses on the polished or grooved implants retrieved from rat bone:

- (1) Small amounts of calcium and phosphate ions were detected on the both types of surfaces, but no calcium phosphate compounds were recognized when considering the Ca/P atomic ratio. Accordingly, the deposition of calcium phosphate cannot be the reason of the excellent biocompatibility of the Ti implant.
- (2) The surface of the retrieved implant was covered with a monolayer of biomolecules including proteins and proteoglycans after 3 hours' implantation. The layer thickness was almost equal between the polished surface and the grooved surface.
- (3) Two binding energies, 163.5 eV and 168 eV, of S 2p were recognized on the both surfaces: The former was assigned to sulfur contained in the cysteine, some of which belonged to BMP. The latter was assigned to sulfur contained in sulfate of organic compound, most of which was from the proteoglycans.
- (4) The amount of sulfur in cysteine was almost equal for both surfaces, but as for sulfur in proteoglycan, the intensity on the polished surface was about two times larger than those on the grooved surface.
- (5) The proteoglycans on the grooved surface contained some amount of calcium ions, thereby indicating performance as a reservoir of Ca.
- (6) In contrast, the proteoglycans on the polished surface contained few calcium ions. This is because most negative charges (sulfate) of the proteoglycan interacted with the mirror positive charges so strongly, and hence, calcium ions were not able to be bound to such a sulfate site.
- (7) Some amounts of Si were detected on the polished surface as a silanolate, but only trace amount was detected on the grooved surface. This result is consistent to the fact that silicon binds to proteoglycans.
- (8) New bone formation was recognized on only the grooved surface. This implies that the grooved surface is more favorable for early bone formation.

Why does the titanium exhibit well-known excellent biocompatibility? The findings in this study indicated that the adsorbed proper biomolecules, such as proteins (including BMP) and proteoglycans, played a vital role.

Why does the proper roughness surface (micron order roughness) exhibit well-known contribution for early bone formation? The findings in this study indicated that proteoglycan played crucial roles for facilitating new bone formation on the Ti surface having a few micron meter texture, and contrarily, did not play roles for bone formation on the polished Ti surface.

ACKNOWLEDGEMENTS

The authors wish to thank all the staff of the Division of Oral Health in Aging and Fixed Prosthodontics, Dept. of Oral Health Science, Course for Oral Life Science, Niigata University Graduate School of Medical and Dental Sciences, for the operation of titanium implant to rat bone. The authors would like to express special appreciation to Dr. Hashimoto, and Mr. Endo, who provided the proper implant samples for the study and arranged the operation procedure including the animal experiments. The authors wish also to thank Dr. Masuda, former professor of the Division of Integrated Manufacturing Systems, School of Science and Technology, Niigata University, for his kind support for fabrication of the grooved Ti surface. This work was financially supported in part by a Grant of City Area Program, Industry-Academia-Government Joint Research Project

Niigata Area (Basic Stage).

REFERENCES

- 1) Jarmar T, Palmquist A, Brånemark R, Hermansson L, Engqvist H, Thomsen P: Characterization of the surface properties of commercially available dental implants using scanning electron microscopy, focused ion beam, and high-resolution transmission electron microscopy. *Clin Implant Dent Relat Res*, 10: 11-22, 2008.
- 2) Jones FH: Teeth and bones: Applications and surface science to dental materials and related biomaterials. *Surface Science Reports* 42. p 75-205, Elsevier, Amsterdam, 2001.
- 3) Hanawa T, Ota M: Calcium phosphate naturally formed on titanium in electrolyte solution. *Biomaterials*, 12: 767-774, 1991.
- 4) Frauchiger L, Taborelli M, Aronsson BO, Descouts P: Ion adsorption on titanium surfaces exposed to a physiological solution. *Appl Surf Sci*, 143: 67-77, 1999.
- 5) Watanabe K, Okawa S, Kanatani M, Homma K: Surface analysis of commercially pure titanium implant retrieved from rat bone. Part 1: Initial biological response of sandblasted surface. *Dent Mater J*, 28: 178-184, 2009.
- 6) Eliades G, Eliades T, Brantley WA, Watts DC: Dental materials in vivo. p 6-7, Quintessence Publishing, Chicago, 2003.
- 7) Vroman L, Adams AL: Finding with the recording ellipsometer suggesting rapid exchange of specific plasma proteins at liquid/solid interfaces. *Surf Sci*, 16: 438-446, 1969.
- 8) Brunette DM, Tengvall P, Textor M, Thomsen P: Titanium in medicine. p 216-217, Springer, Berlin, 2001.
- 9) Guehennec LL, Soueidan A, Layrolle P, Amouriq Y: Surface treatments of titanium dental implants for rapid osseointegration. *Dent Mater*, 23: 844-854, 2007.
- 10) Chehroudi B, McDonnell D, Brunette DM: The effects of micromachined surfaces on formation of bonelike tissue on subcutaneous implants as assessed by radiography and computer image processing. *J Biomed Mater Res*, 34: 279-290, 1997.
- 11) Morra M: Biochemical modification of titanium surface: peptides and ECM proteins. *Eur Cell Mater*, 12: 1-15, 2006.
- 12) Bilezikian JP, Raisz RG, Rodan GA: *Principals of Bone Biology*, 2nd ed, p 225-226, Academic Press, San Diego, 2002.
- 13) Linder L, Albrektsson T, Brånemark PI, Hansson HA, Ivarsson B, Jönsson U, Lundström I: Electron microscope analysis of the bone-titanium interface. *Acta Orthop Scand*, 54: 45-52, 1983.
- 14) Nakamura HK, Butz F, Saruwatari L, Ogawa T: A role for proteoglycans in mineralized tissue-titanium adhesion. *J Dent Res*, 86: 147-152, 2007.
- 15) Bilezikian JP, Raisz RG, Rodan GA: *Principals of bone biology*. 2nd ed, p 365, Academic Press, San Diego, 2002.
- 16) Fujii N, Kusakari H, Maeda T: A histological study on tissue responses to titanium implantation in rat maxilla: the process of epithelial regeneration and bone reaction. *J Periodontol*, 69: 485-495, 1998.
- 17) Tanuma S, Powell CJ, Penn DR: Calculations of electron inelastic mean free paths V. Data for 14 organic compounds over the 50-2000 eV range. *Surf Interface Anal*, 21: 165-176, 1993.
- 18) Sheskin DJ: *Handbook of parametric and nonparametric statistical procedures*. 2nd ed, p 767-776, Chapman & Hall/Crc, Boca Raton, 2000.
- 19) Luth H: *Solid surfaces, interfaces and thin films*. 4th ed, p 69-70, Springer, Berlin, 2001.
- 20) Chastain J, King Jr RC: *Handbook of X-ray photoelectron spectroscopy*. p 253, Physical Electronics Inc, Minnesota, USA, 1995.
- 21) Urban NR, Ernst K, Bernasconi S: Addition of sulfur to organic matter during early diagenesis of lake sediments. *Geochim Cosmochim Acta*, 63: 837-853, 1999.
- 22) Schillinger R, Slijvančanin Z, Hammer B, Greber T: Probing enantioselectivity with X-ray photoelectron spectroscopy and density functional theory. *Phys Rev Lett*, 98: 136102-1-4, 2007.
- 23) Goschnic J, Natzeck C, Sommer M: Depth-resolved analysis of traffic soot sampled in the vicinity of a German motorway. *Surf Interface Anal*, 36: 857-861, 2004.
- 24) Ohare LA, Hynes A, Alexander MR: A

- methodology for curve-fitting of the XPS Si 2p core level from thin siloxane coatings. *Surf Interface Anal*, 39: 926-936, 2007.
- 25) Alberts B, Johnson A, Lewis J Raff M, Roberts K, Walter P: *Molecular biology of the cell*. 4th ed, p 149, Garland Science, New York, 2002.
- 26) Pain RH: *Mechanisms of protein folding*. 2nd ed, p 6-7, Oxford Univ Press, UK, 2000.
- 27) Watanabe K, Hashimoto A, Endo MM: Trace elements on the surface of titanium implants extracted from the rat bone. *Biomed Res Trace Elements*, 15: 262-264, 2004.
- 28) Walsh G: *Proteins biochemistry and biotechnology*. p 3-4, Wiley, New York, 2002.
- 29) Bilezikian JP, Raisz RG, Rodan GA: *Principal of bone biology*. 2nd ed, p 919-920, Academic Press, San Diego, 2002.
- 30) Campagne MV, Thibodeaux H, van Bruggen N, CairnsB, Lowe DG: Increased binding activity at an antioxidant-responsive element in the metallothionein-1 promoter and rapid induction of metallothionein-1 and -2 in response to cerebral ischemia and reperfusion. *J Neurosci*, 20: 5200-5207, 2000.
- 31) Alberts B, Johnson A, Lewis J Raff M, Roberts K, Walter P: *Molecular biology of the cell*. 4th ed, p 1092-1095, Garland Science, New York, 2002.
- 32) Adamson AW: *Physical chemistry of surfaces*. P 520-521, John Wiley & Sons, New York, 1982.
- 33) Jackson JD: *Classical electrodynamics*. 3^d ed, p 57-58, John Wiley & Sons, New York, 1999.
- 34) Bockris JO, Reddy AKN, Gamboa-Aldeco M: *Modern electrochemistry*. Vol 2A, 2nd ed, p 819-821, Kluwer Academic/Plenum Publishers, New York, 2000.
- 35) Hunter GK, Wong KS, Kim JJ: Binding calcium to glycosaminoglycans: An equilibrium dialysis study. *Arch Biochem Biophys*, 260: 161-167, 1988.
- 36) Schwartz NB: Biosynthesis and regulation of expression of proteoglycans. *Front Biosci*, 5: D649-D655, 2000.
- 37) Schwarz K: A bound form of silicon in glycosaminoglycans and polyuronides. *Proc Nat Acad Sci USA*, 70: 1608-1612, 1973.